Available online at www.sciencedirect.com

ScienceDirect

www.elsevier.com/locate/jes

JES JOURNAL OF ENVIRONMENTAL SCIENCES

www.jesc.ac.cn

Novel chitosan–ethylene glycol hydrogel for the removal of aqueous perfluorooctanoic acid

*Li Long, Xiaolan Hu, Jinpeng Yan, Yifan Zeng, Jiaqi Zhang, Yingwen Xue**

School of Civil Engineering, Wuhan University, Wuhan 430000, China

ARTICLE INFO

Article history:
Received 1 February 2019
Revised 9 April 2019
Accepted 10 April 2019
Available online 17 April 2019

Keywords:
PFOA removal
Chitosan-based material
Hydrogel
Adsorption mechanism

ABSTRACT

It is urgent to explore an effective removal method for perfluorooctanoic acid (PFOA) due to its recalcitrant nature. In this study, a novel chitosan-based hydrogel (CEGH) was prepared with a simple method using chitosan and ethylene glycol through a repeated freezing–thawing procedure. The adsorption of PFOA anions to CEGH agreed well to the Freundlich–Langmuir model with a maximum adsorption capacity as high as 1275.9 mg/g, which is higher than reported values of most adsorbents for PFOA. The adsorption was influenced by experimental conditions. Experimental results showed that the main removal mechanism was the ionic hydrogen bond interaction between carbonyl groups (COO^-) of PFOA and protonated amine (NH^+) of the CEGH adsorbent. Therefore, CEGH is a very attractive adsorbent that can be used to remove PFOA from water in the future.

Introduction

Perfluorinated compounds (PFCs) are persistent and toxic organic pollutants that have caused the widespread contamination of soil, ground water and surface water (Milley et al., 2018; Zheng et al., 2017). Because of the chemical and biological stability of C–F bond, PFCs are hard to be decomposed. Perfluorooctanoic acid (PFOA) is one of the most common PFCs and causes a threat to human health because of its reproductive toxicity, neurotoxicity, and immunotoxicity. It can be bioaccumulated and thus be enriched through the food chain. Thus, it is urgent to explore an effective and stable technology to remove PFOA from water.

Several methods have been developed to resolve the contamination of PFOA. Ultraviolet (Zhang et al., 2016b) or photocatalysis (Zhao et al., 2012) can play roles in the degradation of PFCs. Usually PFCs were decomposed into undesirable and negative byproducts, such as F^- and shorter chain perfluorinated compounds that are even more toxic and harder to be treated than the original PFCs. Hydroxyl radical (Gomez-Ruiz et al., 2017) and sulfate radical (Lutze et al., 2017) are used in advanced oxidation process to decompose PFCs. These demonstrated that PFCs could be effectively removed by a series of chemical reactions activated by radicals and the energy consumption and cost required for process of radical generation was significantly high, which was not acceptable for practical application. In addition, Fe(0) (Zhang et al., 2016a), vitamin B12 and Ti(III) (Ochoa-Herrera et al., 2008) are used as electro-donating agents to defluorinate PFCs. However, these defluorination methods of PFCs was limited to their complex operation steps and undesirable removal rates.

Adsorption method has been often used to remove numerous contaminants from different source waters owing to its high efficiency and environment-friendly (e.g., byproduct-free) properties. Therefore adsorption becomes a potential and effective method to remove PFCs. Recently several adsorbents have been used in the removal of PFCs, such as carbon materials (Inyang and Dickenson, 2017; Liu et al., 2018; Sun

* *Corresponding author. E-mail:* ywxue@whu.edu.cn (Yingwen Xue).

https://doi.org/10.1016/j.jes.2019.04.007
1001-0742 © 2019 The Research Center for Eco-Environmental Sciences, Chinese Academy of Sciences. Published by Elsevier B.V.

et al., 2016), nanomaterials (Gong et al., 2016; Wang et al., 2018), polymer materials (Karoyo and Wilson, 2016), and so on. Powdered activated carbon (PAC) combined with persulfate could lead to the chemisorption of PFOA (Sun et al., 2016). PAC was used as the catalyzer to activate the decomposition process of persulfate and then PFOA was removed by reacting with the transformation products. Liu prepared and applied novel starch-stabilized magnetite nanoparticles to remove PFOA (Gong et al., 2016). In his work, the dominate removal mechanism was the inner-sphere surface complexation and after adsorption the biological toxicity of PFOA could be dropped severely. Li synthesized three-metals grafted multi-walled carbon nanotubes (MWCNTs) and used it to remove PFOA (Liu et al., 2018). The results indicated that the intra-particle diffusion well described the adsorption process of PFOA onto the surface of this novel adsorbent and the removal mechanisms were attributed to the hydrophobic interaction, electrostatic attraction, and the formation of the inner sphere complexes. Xu et al. (2015) studied the adsorption of PFOA on polyaniline nanotubes and found the adsorption process of PFOA is endothermic and electrostatic attraction plays the major role on adsorption. Li used mesoporous resin micro-spheres and demonstrated their efficient adsorption perfor-mance for the removal of PFOA (Li et al., 2017).

However, these works still have some shortages, such as high energy requirements and low adsorption capacity. These limit the application of previous works to practical removal of PFOA, which means it is urgent to develop a new method to remove this pollutant. The goal of this work thus is to prepare a novel adsorbent to efficiently remove PFOA without any shortages.

Chitosan is a well-known material derived from natural organic biomass and has obtained global attention for its unique physicochemical properties. The chemical name of chitosan is known as poly[2-amino-2-deoxy-d-glucose]. This organic material is able to be modified or combined with other materials, which is beneficial for its various applications in environmental field. Due to the plentiful source extracted from crustacean shells, including crab and shrimp shells, and fungal mycelia, chitosan possesses more potential for diverse applications (Wang et al., 2017). To be identified as economic adsorbent, the preparation and application of a certain type of material ought to require easy processing steps, consume little energy, have abundant sources from nature and possess byproduct-free ability (Bailey et al., 1999). Therefore chitosan material meets these requirements and is widely acknowledged to be a low-cost feedstock to develop novel adsorbents. Among diverse chitosan-based materials, chito-san hydrogels are emerging adsorbents for various contami-nants, such as heavy metals (Wang et al., 2014), antibiotics (Afzal et al., 2018), and dyes (Rashid et al., 2018). However, chitosan-based hydrogels have not been applied to remove PFOA from water and it is advisable to prepare hydrogels with little toxicity.

So the objectives of this work are as follows: (1) apply a novel chitosan-based hydrogel with simple preparation to remove PFOA; (2) explore the adsorption mechanism of PFOA onto this chitosan-based hydrogel; and (3) determine the effect of different influencing factors on adsorption process of PFOA.

1. Materials and methods

1.1. Materials

All materials in this work were used as purchased without the least extraction or purification. Chitosan, ethylene glycol (EG, 99%), ammonia solution ($NH_3{\cdot}H_2O$, 25%–28%), glacial acetic acid (99.5%), and ammonium acetate (NH_4AcO) were all purchased from Sinopharm Chemical Reagent Co., Ltd. PFOA (100%) was bought from Aladdin Chemical Reagent Co., Ltd. High performance liquid chromatography (HPLC)-grade ace-tonitrile (ACN) was obtained from Merck KGaA (Germany). The PFOA solutions were prepared by dissolving the solid sample in deionized water.

1.2. Hydrogel production

Chitosan–ethylene glycol hydrogel was synthesized using the repeated freezing–thawing procedure, which is one of the popular methods to prepare hydrogels. The detailed process is as follows. Diluted acetic acid (2% (V/V)) was prepared and then chitosan (5 g) was dissolved in this acid solution (100 mL) at 70°C under magnetic stirring till the chitosan solution became transparent. Then, 20 mL EG solution was added into chitosan solution under continuous stirring at 50°C for 20 min, followed by pouring into molds. The mixture solution was frozen at −20°C for 11 hr and then thawed at room temperature (25°C) for 1 hr. This freezing–thawing process was repeated five times to prepare hydrogel. After that hydrogel was vacuum dried at 45°C for 4 hr and then oven dried at 60°C for 20 hr. Finally, the chitosan–ethylene glycol hydrogel (CEGH) was successfully prepared and cut into 4 mm × 4 mm fragments for later experiments.

1.3. Characterizations

CEGH was characterized with several equipments and facili-ties. Scanning electron microscopy (SEM, JEM-6700F, Hitachi Limited, Japan) was used to determine the surface morphol-ogy. Fourier transform infra-red spectroscopy (FT-IR, NICOLET 5700, Thermo Electron Corporation, USA) was applied to test the functional groups. X-ray photoelectron spectrometry (XPS) was conducted to analyze the surface elemental composition and speciation (Thermo Fisher Company, ESCALAB 250Xi).

1.4. Batch adsorption

PFOA adsorption performance was studied by batch experi-ments with an adsorbent loading of 1 g/L without pH adjustment. 20 mg of CEH was dispersed in 20 mL of PFOA solution with various concentration (100–2000 mg/L), followed by shaking (120 r/min) at 30°C for 24 hr to achieve adsorption equilibrium. Then the mixture was filtered through 0.22 μm membrane filter to achieve solid–liquid separation. A HPLC-evaporative light scattering detector (HPLC-ELSD) system was used to determine the concentration of PFOA. This system consisted of a Shimadzu (Tokyo, Japan), LC-20AD pump, a Thermo HPLC column (4.6 × 150 mm, 5 μm, USA), and an Alltech 2000 ES ELSD (Grace, USA). The mobile phase was 45%

NH_4AcO (10 mmol/L)–55% ACN at a flow rate of 0.5 mL/min and a column oven of 40°C. In the ELSD system, the temperature of drift tube was 95°C and the flow rate of carrier gas (N_2) was 2.4 mL/min produced from a WSK-A auto air generator (Tianjin, China).

Adsorption capacity q (mg/g) of PFOA on CEGH and the removal rate R (%) were calculated based on difference between the initial and final aqueous concentrations. The calculation used following mathematic equations:

$$q = \frac{(C_0 - C_e)V}{m} \quad (1)$$

where C_0 (mg/L) and C_e (mg/L) represent the initial and equilibrium PFOA concentration, respectively. V (L) is the volume of the PFOA solution and m (g) is the amount of adsorbent.

1.5. Effects of pH and reaction temperature

The effects of pH and reaction temperature on the adsorption process of PFOA were studied. To investigate the influence of pH on adsorption, the initial pH of PFOA solutions (1200 mg/L) was adjusted to a certain value by using diluted HAc and $NH_3{\cdot}H_2O$ (0.01, 1, and 100 mmol/L). Different reaction temperature, ranging from 20 to 40°C, was also studied to determine the effect of temperature.

1.6. Mathematical models

Adsorption isotherms were obtained from the adsorption amount at different initial PFOA concentrations. These concentrations were changed from 400 to 2000 mg/L. Langmuir, Freundlich, and Langmuir–Freundlich models were used to simulate the isotherms and their governing equations can be described as (Yan et al., 2018):

$$\text{Langmuir}: q_e = \frac{KS_{max}C}{1 + KC} \quad (2)$$

$$\text{Freundlich}: q_e = K_F C^n \quad (3)$$

$$\text{Langmuir–Freundlich}: q_e = \frac{S_{max}(K_{LF}C)^n}{1 + (K_{LF}C)^n} \quad (4)$$

where K (L/mg), K_F ((mg/g) (1/mg)$^{1/n}$) and K_{LF} (L/mg) are the Langmuir constant, the Freundlich affinity coefficient, and Langmuir–Freundlich constant, respectively. C (mg/L) is the equilibrium solution concentration of the sorbate. S_{max} (mg/g) is the Langmuir maximum capacity and n is the Freundlich linearity constant.

Sorption kinetics of PFOA were assessed by measuring the adsorption capacity at different time (2, 4, 6, 8, 10, 12, 16, 20, and 24 hr). Pseudo first-order, pseudo second-order, and Elovich models were used to simulate the sorption kinetics data. Governing equations of these models can be written as (Inyang et al., 2012):

$$\text{Pseudo first–order}: q_t = q_e\left(1 - e^{-k_1 t}\right) \quad (5)$$

$$\text{Pseudo second–order}: q_t = \frac{k_2 q_e^2 t}{1 + k_2 q_e t} \quad (6)$$

$$\text{Elovich}: q_t = \frac{1}{\beta}\ln(\alpha\beta t + 1) \quad (7)$$

where q_t (mg/g) and q_e (mg/g) represent the amounts of PFOA adsorbed at contact time t (hr) and at equilibrium, respectively. k_1 (hr^{-1}) and k_2 (hr^{-1}) are the rate constants of pseudo first-order and pseudo second-order model, respectively. α (mg/g) is the initial sorption rate and β (g/mg) is the desorption constant.

2. Results and discussion

2.1. Hydrogel characterization

There were obvious changes in element content after adsorption of PFOA. C content slightly increased from 72.28% to 74.15%, suggesting PFOA were adsorbed on CEGH because each PFOA molecule has eight carbon atoms. Notably, before

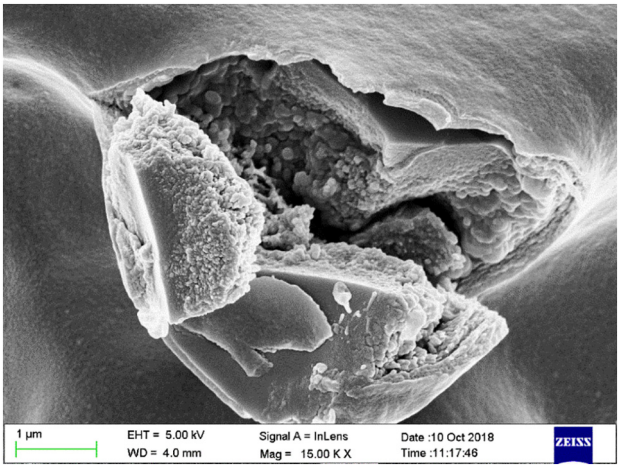

Fig. 1 – The scanning electron micrograph (SEM) of CEGH.

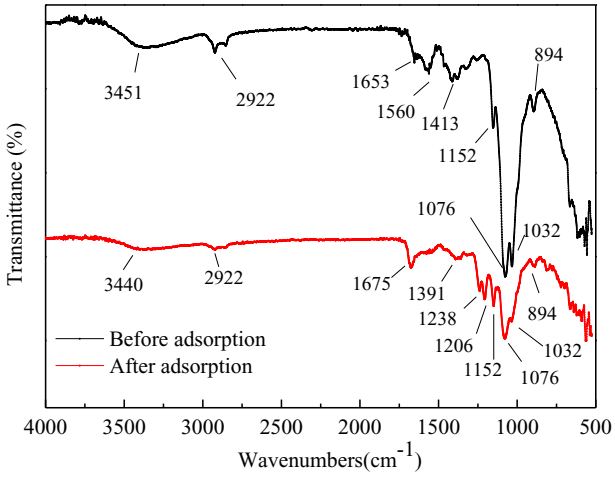

Fig. 2 – FTIR spectra of CEGH before and after adsorption.

adsorption CEGH did not contained F element but after adsorption there was a significant increase of F element content (up to 7.2%). Taking PFOA rich in F element into consideration, this result firmly proved that CEGH was an effective adsorbent to PFOA.

Fig. 1 depicted the surface morphology of CEGH, showing a rough surface when the magnification was ×15,000. In the preparation process, repeated freezing–thawing procedure made the hydrogel more homogeneous. Drying process removed volatile components, leading to the rough surface morphology. This property was fundamental because the rough surface morphology was beneficial for adsorption process, which has been demonstrated in previous studies (Long et al., 2017; Zhao et al., 2018).

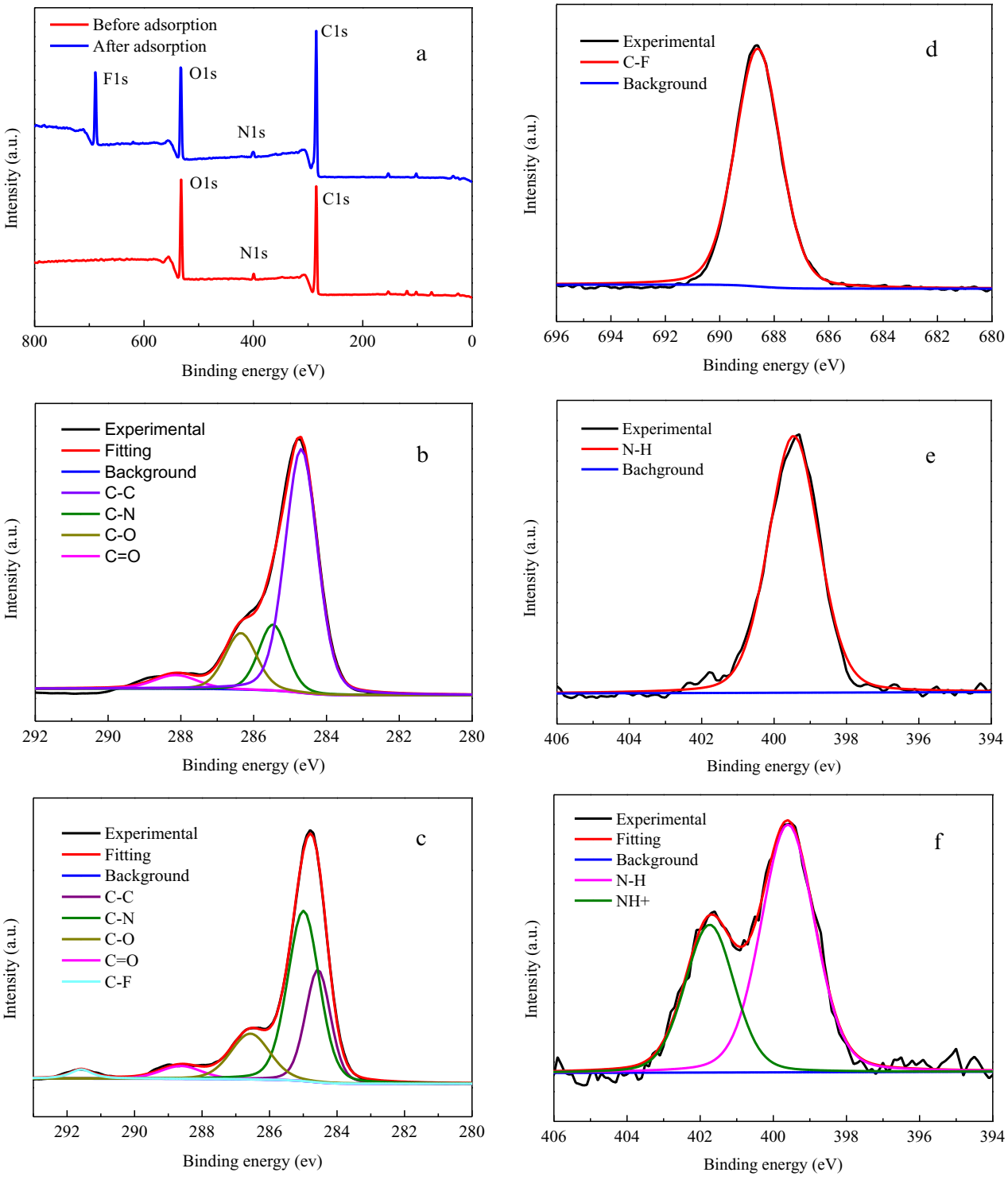

Fig. 3 – XPS spectra of CEGH before and after the adsorption of PFOA.

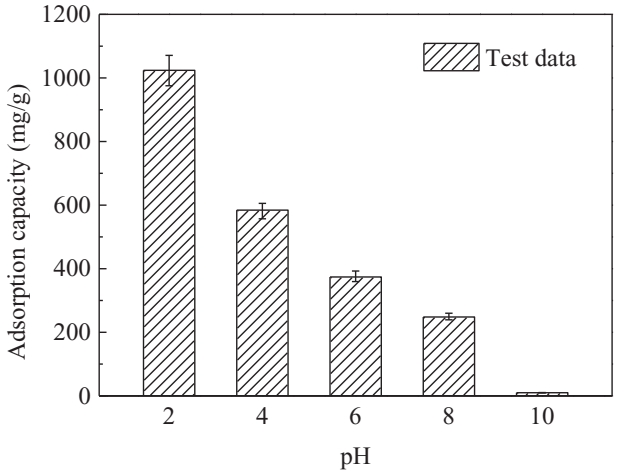

Fig. 4 – Effect of pH on PFAA adsorption onto CEGH.

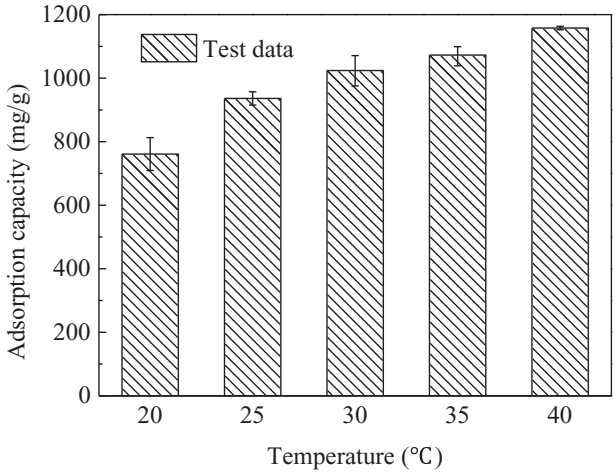

Fig. 5 – Effect of temperature on PFOA adsorption onto CEGH.

As the data shown in Fig. 2, several peaks were attributed to different surface functional groups in CEGH. The broad band around 3251 cm^{-1} could be assigned to be overlapping N–H and O–H (Deng et al., 2017; Yazdani et al., 2017), and the peak at 2922 cm^{-1} might be assigned to the hydroxyl group (O–H) (Hu et al., 2018b). The peaks at 1653, 1560 and 1413 cm^{-1} were attributed to the typical spectrums of amide groups (CONH) (Guaresti et al., 2017; Zhu et al., 2019). The peaks at around 1152 and 894 cm^{-1} were resulted from β glycosidic bond of chitosan (Vasilieva et al., 2017). The obvious signals at around 1076 and 1032 cm^{-1} were typical of C–C and C–O bond (Hu et al., 2018a). These FT-IR spectra characterizations of the prepared CEGH agreed well with previously reported chitosan-based materials (Vasilieva et al., 2017; Zhu et al., 2019). After adsorption, several different and new peaks were represented. The intensity of the peak at around 1675 cm^{-1} increased, which belonged to C=O band, suggesting the efficient adsorption of PFOA on CEGH due to the carboxyl group PFOA possessed in the aqueous condition. The new and sharp peaks at 1238 and 1206 cm^{-1} could be attributed to C–F bond (Luo et al., 2018) of PFOA. The intensity of peaks corresponding N–H changed to lower wavenumbers, suggesting N–H may play a role in adsorption of PFOA. All these demonstrated the interaction between CEGH and PFOA, conforming the effective adsorption.

As shown in Fig. 3, XPS was used to determine the chemical compositions of CEGH before and after adsorption. Fig. 3a showed a new and strong peak of F1s at around 688.6 eV emerged after adsorption, suggesting PFOA was effectively adsorbed. Fig. 3b and c represented that C1s had four different peaks. Peak C1 (at 284.6 eV), peak C2 (at 285.4 and 285.1 eV), peak C3 (at 286.4 and 286.5 eV) and peak C4 (at 288.2 and 288.6 eV) could be respectively assigned to the carbon atoms of C–C, C–N, C–O, and C=O (Deng et al., 2017; Dorraki et al., 2015; Fan et al., 2018; Kumar et al., 2017). After adsorption, there was a new peak C5 (at 291.6 eV) for C–F bond (Fig. 3d) (Fan et al., 2018). The F1s spectrum of CEGH after adsorption contained the C–F bonds at about 688.6 eV (Fan et al., 2018). These results confirmed the adsorption of PFOA onto CEGH. In addition, Fig. 3e and f indicated the nitrogen XPS spectra of CEGH. Before adsorption, this adsorbent only contained non-protonated amine (N–H) at around 399.5 eV (Deng et al., 2017; Mighri et al., 2015). But after adsorption, a new peak emerged at around 401.7 eV, which was typical to NH^+ (Dorraki et al., 2015; Mighri et al., 2015), a protonated amine. NH^+ was such a positive molecule that was easy to lead to the formation of ionic hydrogen bond interactions with carbonyl groups (COO^-) of PFOA (Li et al., 2017), fundamentally improving adsorption ability of CEGH.

2.2. Effects of pH and adsorption temperature

The initial pH value of sample solution and reaction temperature played vital roles in adsorption process of anion removal (Hu et al., 2018a). Fig. 4 displayed the variation tendency of adsorption capacity of PFOA with the different initial pH, from 2 to 10. As the pH of PFOA solution increased, the adsorption capacity decreased significantly. PFOA always existed as a carbonyl anion in the solution (Li et al., 2017). At the pH of 2, the adsorption capacity reached the highest, up to 1024 mg/g, probably because ionic hydrogen bond interactions between carbonyl groups in PFOA and protonated amine (NH^+) in the CEGH adsorbent dominated the adsorption in low pH. The increase of initial pH was attributed to weaken the

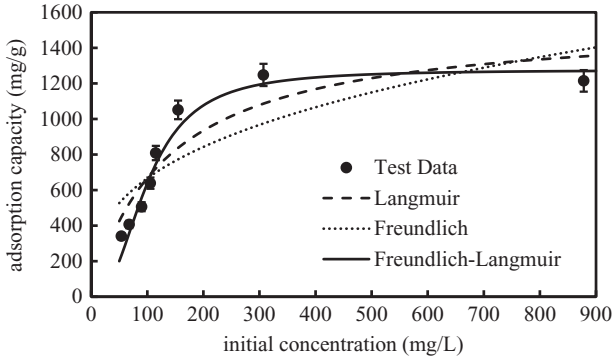

Fig. 6 – Isotherm of PFOA adsorption onto CEGH.

Table 1 – Isotherm parameters of PFOA adsorption onto CEGH.

Adsorbent	Langmuir			Freundlich			Freundlich- Langmuir			
	S_{max}	K	R^2	K_F	n	R^2	S_{FL}	K_{FL}	n_{FL}	R^2
CEGH	1557.52	0.0075	0.845	139.788	0.339	0.684	1275.9	0.01	2.43	0.964

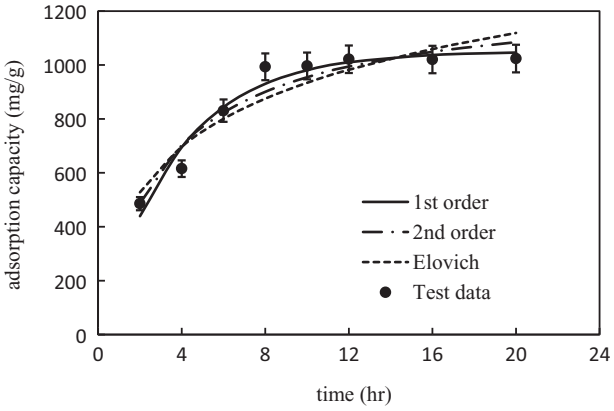

Fig. 7 – Kinetics of PFOA adsorption onto CEGH.

ionic hydrogen bond, reducing the adsorption capacity of PFOA. When pH reached 8, the alkaline condition was unfavorable to the adsorption of PFOA. Notably, at the pH of 10, the adsorption capacity was near 0 mg/g, probably because large amount of OH^- in strong alkaline condition was much easier to form the ionic hydrogen bond interactions than carbonyl groups in PFOA.

As shown in Fig. 5, the influence of temperature on adsorption of PFOA was obvious. With the increasing temperature from 20 to 40°C, the adsorption capacity increased correspondently, which may be attributed to the mass transfer activated by a higher temperature. When temperature was over 30°C, the adsorption capacity increased slightly, up to 1158 mg/g. This phenomenon could be made full use of in the practical application so that the adsorption rate of PFOA could keep high.

Table 2 – Kinetic parameters of PFOA adsorption onto CEGH.

Kinetics	Parameters				
	q_e (mg/g)	k (hr^{-1})	α (g/mg)	β (mg/g)	R^2
Pesudo-first-order	1050.83	0.271	–	–	0.96
Pseudo-second-order	1255.74	0.000252	–	–	0.927
Elovich	–	–	806.23	0.00366	0.875

2.3. Adsorption kinetics and isotherms

To understand the adsorption behavior, the adsorption isotherms of PFOA on the CEGH were shown in Fig. 6. The Langmuir, Freundlich, and Freundlich–Langmuir(F–L) models were applied to fit the data and the resulting parameters were given in Table 1. The isotherm data were better fit by the Freundlich–Langmuir model, which had a R^2 (0.964) close to 1. The correlation coefficients of Langmuir and Freundlich model were 0.845 and 0.684, respectively. Based on the Freundlich–Langmuir model, the maximum sorption capacity was 1275.9 mg/g. This was much higher than the adsorption capacities of other adsorbents in previous studies (Li et al., 2017; Sun et al., 2016).

The sorption kinetics were conducted to explore PFOA adsorption process by CEGH. Fig. 7 illustrated the changes in the adsorption capacity as a function of contact time at initial concentration of 1200 mg/L. There was a rapid PFOA adsorption occurred within the first 8 hr, followed by a slower adsorption stage until the equilibrium was reached at 10 hr. The experiment data were fitted with widely used kinetic models, including pseudo first-order, pseudo second-order, and Elovich models. And the corresponding kinetic parameters were summarized in Table 2. Pseudo first-order model had the best fit with R^2 of 0.96, higher than those of the other two models.

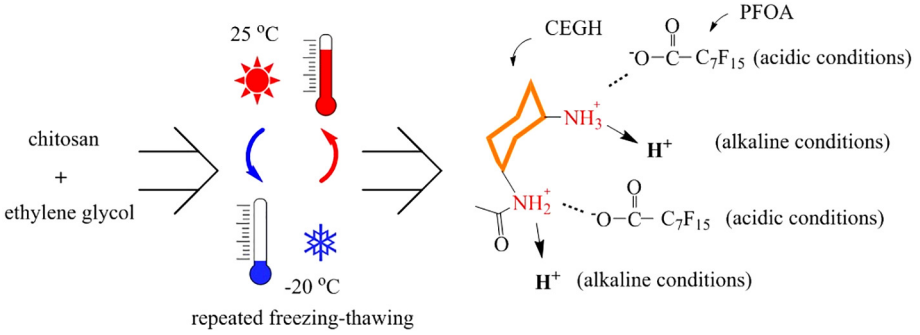

Fig. 8 – Governing mechanisms of PFOA adsorption onto CEGH.

2.4. Adsorption mechanism

The experimental results clearly showed that protonated amine led to ionic hydrogen bond of PFOA onto CEGH. As observed in FTIR analysis (Fig. 2), N–H group played a role in the adsorption. Additionally, XPS spectra (Fig. 3) showed a new peak of protonated amine groups (NH^+). In acidic condition, the amine groups of CEGH was able to be protonated. In this protonation process, it was easy to take place nucleophilic addition. H^+ was active enough to attack the lone pair electrons of amine, classified as nucleophile group. This chemical reaction generated a center with positive charge that was identified as electrophile group, which was favorable to adsorb anion in the aqueous environment (Sohbatzadeh et al., 2017). As a result, the ionic hydrogen bond between carbonyl groups (COO^-) in PFOA and protonated amine (NH^+) in the CEGH adsorbent could be able to take place, leading to the high adsorption capacity of PFOA onto CEGH. As shown in Fig. 4, when pH was lower, ionic hydrogen bond was stronger to maintain the higher adsorption; while under the alkaline condition, few amine groups on the surface of the adsorbent were protonated so that the adsorption dropped remarkably (nearly 0 mg/g at the pH of 10). The governing mechanism of the adsorption of PFOA anions on CEGH was well described in Fig. 8.

3. Conclusion

In this study, a novel chitosan-based hydrogel was prepared from chitosan and ethylene glycol following the repeated freezing–thawing procedure. It effectively removed PFOA from water under acidic conditions. The adsorption process agreed well with the simulation of the Freundlich–Langmuir model with the maximum adsorption capacity of 1275.9 mg/g. The adsorption was strongly affected by experimental conditions include solution pH and temperature. Based on the characterization data, the governing mechanism of PFOA adsorption onto CEGH was determined and the ionic hydrogen bond interaction dominated the removal process. Therefore, CEGH was a very desirable adsorbent and possessed a potential environmental application for PFOA removal from wastewater.

Acknowledgments

This work was partially supported by the Wuhan Water Engineering & Technology Co. Ltd. The authors also thank the anonymous reviewers for their invaluable insight and helpful suggestions.

REFERENCES

Afzal, M.Z., Sun, X.F., Liu, J., Song, C., Wang, S.G., Javed, A., 2018. Enhancement of ciprofloxacin sorption on chitosan/biochar hydrogel beads. Sci. Total Environ. 639, 560–569.

Bailey, S.E., Olin, T.J., Bricka, R.M., Adrian, D.D., 1999. A review of potentially low-cost sorbents for heavy metals. Water Res. 33, 2469–2479.

Deng, J., Liu, Y., Liu, S., Zeng, G., Tan, X., Huang, B., et al., 2017. Competitive adsorption of Pb(II), Cd (II) and Cu (II) onto chitosan-pyromellitic dianhydride modified biochar. J. Colloid Interface Sci. 506, 355–364.

Dorraki, N., Safa, N.N., Jahanfar, M., Ghomi, H., Ranaei-Siadat, S.O., 2015. Surface modification of chitosan/PEO nanofibers by air dielectric barrier discharge plasma for acetylcholinesterase immobilization. Appl. Surf. Sci. 349, 940–947.

Fan, K., Liu, J., Wang, X., Liu, Y., Lai, W.C., Gao, S.S., et al., 2018. Towards enhanced tribological performance as water-based lubricant additive: selective fluorination of graphene oxide at mild temperature. J. Colloid Interface Sci. 531, 138–147.

Gomez-Ruiz, B., Ribao, P., Diban, N., Rivero, M.J., Ortiz, I., Urtiaga, A., 2017. Photocatalytic degradation and mineralization of perfluorooctanoic acid (PFOA) using a composite TiO_2 -rGO catalyst. J. Hazard. Mater. 344, 950–957.

Gong, Y., Wang, L., Liu, J., Tang, J., Zhao, D., 2016. Removal of aqueous perfluorooctanoic acid (PFOA) using starch-stabilized magnetite nanoparticles. Sci. Total Environ. 562, 191–200.

Guaresti, O., García–Astrain, C., Palomares, T., Alonso–Varona, A., Eceiza, A., Gabilondo, N., 2017. Synthesis and characterization of a biocompatible chitosan–based hydrogel cross–linked via 'click' chemistry for controlled drug release. Int. J. Biol. Macromol. 102.

Hu, X., Xue, Y., Long, L., Zhang, K., 2018a. Characteristics and batch experiments of acid- and alkali-modified corncob biomass for nitrate removal from aqueous solution. Environ. Sci. Pollut. Res. 1–9.

Hu, X.L., Xue, Y.W., Liu, L.N., Zeng, Y.F., Long, L., 2018b. Preparation and characterization of Na2S-modified biochar for nickel removal. Environ. Sci. Pollut. Res. 25, 9887–9895.

Inyang, M., Dickenson, E.R.V., 2017. The use of carbon adsorbents for the removal of perfluoroalkyl acids from potable reuse systems. Chemosphere 184, 168–175.

Inyang, M., Gao, B., Yao, Y., Xue, Y.W., Zimmerman, A.R., Pullammanappallil, P., et al., 2012. Removal of heavy metals from aqueous solution by biochars derived from anaerobically digested biomass. Bioresour. Technol. 110, 50–56.

Karoyo, A.H., Wilson, L.D., 2016. Investigation of the adsorption processes of fluorocarbon and hydrocarbon anions at the solid–solution interface of macromolecular imprinted polymer materials. J. Phys. Chem. C 120.

Kumar, S., Gonen, S., Freidman, A., Elbaz, L., Nessim, G.D., 2017. Doping and reduction of graphene oxide using chitosan-derived volatile N-heterocyclic compounds for metal-free oxygen reduction reaction. Carbon 120.

Li, J., Li, Q., Li, L.S., Xu, L., 2017. Removal of perfluorooctanoic acid from water with economical mesoporous melamine-formaldehyde resin microsphere. Chem. Eng. J. 320.

Liu, L., Li, D., Li, C., Ji, R., Tian, X., 2018. Metal nanoparticles by doping carbon nanotubes improved the sorption of perfluorooctanoic acid. J. Hazard. Mater. 351, 206.

Long, L., Xue, Y., Zeng, Y., Yang, K., Lin, C., 2017. Synthesis, characterization and mechanism analysis of modified crayfish shell biochar possessed ZnO nanoparticles to remove trichloroacetic acid. J. Clean. Prod. 166, 1244–1252.

Luo, L.B., Hong, D.W., Zhang, L.J., Cheng, Z., Liu, X.Y., 2018. Surface modification of PBO fibers by direct fluorination and corresponding chemical reaction mechanism. Compos. Sci. Technol. 165, 106–114.

Lutze, H.V., Brekenfeld, J., Naumov, S., Sonntag, C.V., Schmidt, T. C., 2017. Degradation of perfluorinated compounds by sulfate radicals – new mechanistic aspects and economical considerations. Water Res. 129, 509–519.

Mighri, N., Mao, J.F., Mighri, F., Ajji, A., Rouabhia, M., 2015. Chitosan-coated collagen membranes promote chondrocyte adhesion, growth, and interleukin-6 secretion. Materials 8, 7673–7689.

Milley, S.A., Koch, I., Fortin, P., Archer, J., Reynolds, D., Weber, K.P., 2018. Estimating the number of airports potentially

contaminated with perfluoroalkyl and polyfluoroalkyl substances from aqueous film forming foam: a Canadian example. J. Environ. Manag. 222, 122–131.
Ochoa-Herrera, V., Sierra-Alvarez, R., Somogyi, A., Jacobsen, N.E., Wysocki, V.H., Field, J.A., 2008. Reductive defluorination of perfluorooctane sulfonate. Environ. Sci. Technol. 42, 3260–3264.
Rashid, S., Shen, C.S., Yang, J., Liu, J.S., Li, J., 2018. Preparation and properties of chitosan-metal complex: some factors influencing the adsorption capacity for dyes in aqueous solution. J. Environ. Sci. 66, 301–309.
Sohbatzadeh, H., Keshtkar, A.R., Safdari, J., Yousefi, T., Fatemi, F., 2017. Insights into the biosorption mechanisms of U(VI) by chitosan bead containing bacterial cells: a supplementary approach using desorption eluents, chemical pretreatment and PIXE-RBS analyses. Chem. Eng. J. 323, 492–501.
Sun, B., Ma, J., Sedlak, D.L., 2016. Chemisorption of perfluorooctanoic acid on powdered activated carbon initiated by persulfate in aqueous solution. Environ. Sci. Technol. 50, 7618.
Vasilieva, T., Chuhchin, D., Lopatin, S., Varlamov, V., Sigarev, A., Vasiliev, M., 2017. Chitin and cellulose processing in low-temperature electron beam plasma. Molecules 22.
Wang, H.L., Tang, H.Q., Liu, Z.T., Zhang, X., Hao, Z.P., Liu, Z.W., 2014. Removal of cobalt(II) ion from aqueous solution by chitosan-montmorillonite. J. Environ. Sci. 26, 1879–1884.
Wang, W.Y., Zhao, S., Yue, Q.Y., Gao, B.Y., Song, W., Feng, L.J., 2017. Purification, characterization and application of dual coagulants containing chitosan and different Al species in coagulation and ultrafiltration process. J. Environ. Sci. 51, 214–221.
Wang, W., Xu, Z., Zhang, X., Wimmer, A., Shi, E., Qin, Y., et al., 2018. Rapid and efficient removal of organic micropollutants from environmental water using a magnetic nanoparticles-attached fluorographene-based sorbent. Chem. Eng. J. 343, 61–68.
Xu, C., Chen, H., Jiang, F., 2015. Adsorption of perflourooctane sulfonate (PFOS) and perfluorooctanoate (PFOA) on polyaniline nanotubes. Colloids Surf. A Physicochem. Eng. Asp. 479, 60–67.
Yan, J., Xue, Y., Long, L., Zeng, Y., Hu, X., 2018. Adsorptive removal of As(V) by crawfish shell biochar: batch and column tests. Environ. Sci. Pollut. Res. Int. 25, 34674–34683.
Yazdani, M., Bhatnagar, A., Vahala, R., 2017. Synthesis, characterization and exploitation of nano-TiO2/feldspar-embedded chitosan beads towards UV-assisted adsorptive abatement of aqueous arsenic (As). Chem. Eng. J. 316, 370–382.
Zhang, L.H., Cheng, J.H., You, X., Liang, X.Y., Hu, Y.Y., 2016a. Photochemical defluorination of aqueous perfluorooctanoic acid (PFOA) by Fe 0/GAC micro-electrolysis and VUV-Fenton photolysis. Environ. Sci. Pollut. Res. 23, 13531–13542.
Zhang, T.L., Pan, G., Zhou, Q., 2016b. Temperature effect on photolysis decomposing of perfluorooctanoic acid. J. Environ. Sci. 42, 126–133.
Zhao, B.X., Lv, M., Zhou, L., 2012. Photocatalytic degradation of perfluorooctanoic acid with beta-Ga2O3 in anoxic aqueous solution. J. Environ. Sci. 24, 774–780.
Zhao, H., Xue, Y., Long, L., Hu, X., 2018. Adsorption of nitrate onto biochar derived from agricultural residuals. Water Sci. Technol. wst2017568.
Zheng, B.H., Liu, X.L., Guo, R., Fu, Q., Zhao, X.R., Wang, S.J., et al., 2017. Distribution characteristics of poly- and perfluoroalkyl substances in the Yangtze River Delta. J. Environ. Sci. 61, 97–109.
Zhu, L.F., Li, J.S., Mai, J., Chang, M.W., 2019. Ultrasound-assisted synthesis of chitosan from fungal precursors for biomedical applications. Chem. Eng. J. 357, 498–507.